Building the Northern Tien Shan: Integrated Thermal, Structural, and Topographic Constraints

M. E. Bullen,[1] *D. W. Burbank,*[2] *and J. I. Garver*[3]

Department of Geosciences, Pennsylvania State University, State College, Pennsylvania 16801, U.S.A.
(*e-mail: mebulle@msn.com*)

ABSTRACT

Paired apatite fission track and U-Th/He dates provide the first Late Cenozoic cooling ages for the northern Tien Shan. These data clearly argue for pulsed deformation since the Late Miocene, with early (10–11 Ma) and late (0–3 Ma) intervals of rapid exhumation separated by an extended interval of much slower rates. By integrating these bedrock cooling rates with shortening estimates derived from a balanced section, detrital cooling ages, and geomorphological estimates of conditions before deformation, we reconstruct a four-stage history of range growth and exhumation. Following ~100 m.yr. of tectonic quiescence, abruptly accelerated rock uplift, exhumation, and cooling in the Kyrgyz Range commenced at ~11 Ma with rates exceeding ~1 km/m.yr. During the subsequent 7 m.yr., deformation and cooling rates decreased three- to sixfold before accelerating by comparable amounts during the past 3 m.yr. Since mid-Miocene times, the surface elevation of the Kyrgyz Range has increased ~2 km, consistent with the reconstructed magnitude of crustal shortening (~11 km) and thickening (~12 km) across the range. The highly pulsed deformation rates indicate that the locus of deformation probably shifted repeatedly within the Tien Shan from the Miocene to present. Even at their most rapid, Cenozoic shortening rates in the Kyrgyz Range were equivalent to only 10%–20% of the modern geodetic convergence rate across the entire Tien Shan. This requires several ranges within the Tien Shan to have deformed simultaneously since the Middle Miocene, a situation analogous to the distributed shortening seen today.

Introduction

Despite the striking topography of the Himalaya and adjacent Tibetan Plateau, nearly half of the present-day Indo-Asian convergence is absorbed by deformation some 1000–2000 km north, within the interior ranges of Central Asia (fig. 1). Geodetic studies indicate that the present shortening rate in the Tien Shan (~20–23 km/m.yr.; Abdrakhmatov et al. 1996; Wang et al. 2000; Reigber et al. 2001) is equivalent to the shortening rate across the main Himalaya (Larson et al. 1999). Rapid shortening in the Tien Shan has created the highest summits outside of the Himalaya and makes this range a quintessential example of intracontinental mountain building. Study of the Tien Shan also provides a unique opportunity to evaluate unanswered issues regarding deformation in Central Asia, such as the style and timing of strain propagation and the causal relationship between uplift of the Tibetan Plateau and development of the Tien Shan.

The timing of the initial growth of the Tien Shan, however, remains controversial. Magnetostratigraphic sections and fission track ages in the eastern and southern Tien Shan indicate that erosional exhumation of these ranges began at 20–25 Ma (Hendrix et al. 1994; Sobel and Dumitru 1997; Yin et al. 1998) and may have been linked to a switch from extrusion-dominated to crustal-thickening-dominated tectonics (Hendrix et al. 1994; Sobel and Dumitru 1997). Alternatively, initial Tien Shan growth has been estimated at ~10 Ma on the basis of extrapolation of the geodetic shortening rate, given that the total Cenozoic shortening across the Tien Shan has been estimated at 200 ± 50 km (Avouac et al. 1993; Abdrakhmatov et al. 1996). It

Manuscript received August 16, 2001; accepted August 8, 2002.

[1] Present address: ExxonMobil Exploration Company, GP3, Benmar Street, Houston, Texas 77060, U.S.A.

[2] Present address: Department of Geological Sciences, University of California, Santa Barbara, Building 526, Santa Barbara, California 93106-9630, U.S.A.

[3] Geology Department, Olin Building, Union College, Schenectady, New York 12308, U.S.A.

[The Journal of Geology, 2003, volume 111, p. 149–165] 0022-1376/2003/11102-0002$15.00

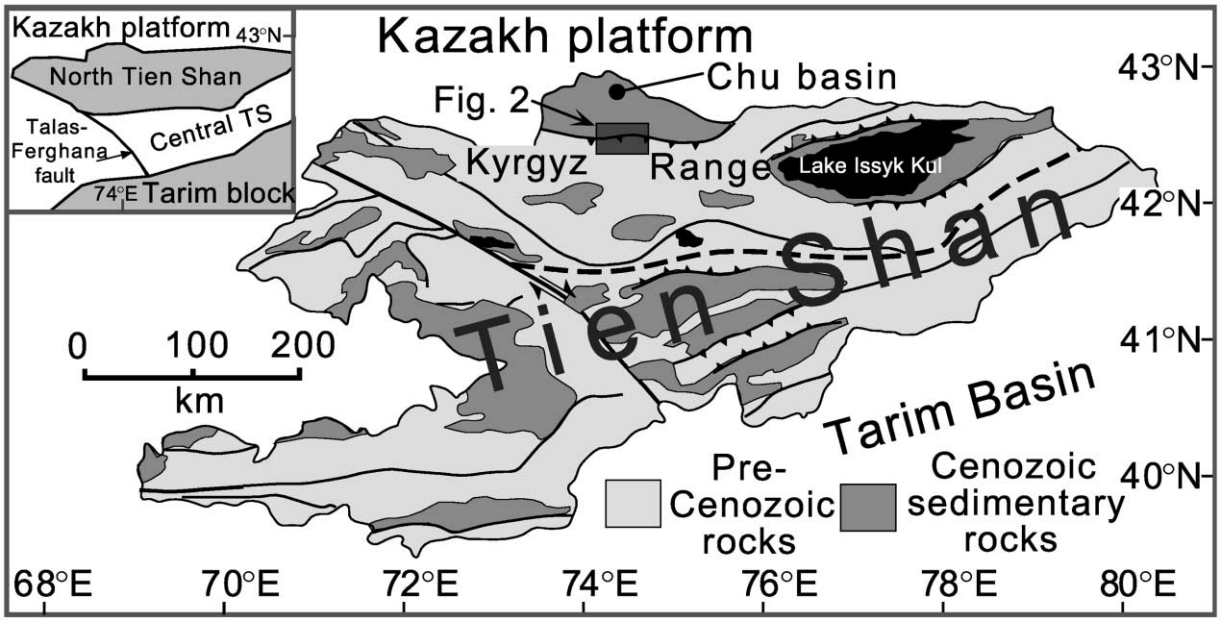

Figure 1. Generalized geologic map of the Kyrgyz Tien Shan, showing major east-west-trending structural features and geologic provinces. Inset shows the large-scale tectonic blocks within and flanking the Kyrgyz Tien Shan.

has been speculated that the proposed initial growth of the Tien Shan at 10 Ma is tectonically linked to the rise of the Tibetan Plateau (Molnar et al. 1993; Abdrakhmatov et al. 1996). Revised shortening estimates across the Kyrgyz Tien Shan (40–80 km; Abdrakhmatov et al. 2001), when combined with the geodetic rate across the same transect (Abdrakhmatov et al. 1996), suggest that deformation initiated at 3–7 Ma.

Not only is the timing of deformation poorly known in the Kyrgyz Tien Shan but also there are many unanswered questions regarding the magnitude, style, and rate of shortening. For example, once shortening began, did it proceed steadily or in pulses (Meigs 1997)? Do the aprons of coarse clastic debris found at the margins of the ranges of the Tien Shan represent accelerated Quaternary erosion (Zhang et al. 2001) or the propagation of shortening and rock uplift into the foreland (Zheng 2000)? Is the magnitude of total Cenozoic shortening and erosion consistent with the inferred changes in crustal thickness in this region (Roecker 1999)? Did the entire range begin to grow in Early Miocene, consistent with ages in the southern Tien Shan, or was initiation diachronous?

In this study, we combine low-temperature thermochronologic data from both the mountainous hinterland and adjacent basins with structural mapping and topographic analysis to provide initial answers to the questions posed above. We focus on the Kyrgyz Range because it represents the northernmost major range of the western Tien Shan and is likely to provide an important perspective regarding the onset and subsequent distribution of deformation throughout the Tien Shan.

Tectonic Setting

Two Paleozoic collisional events occurred in the Tien Shan: one along the southern margin of the range (Late Devonian–Early Carboniferous) and a second along the northern margin (Late Carboniferous–Early Permian; Burtman 1975; Windley et al. 1990; Allen et al. 1993; Carroll et al. 1995). The former involved the collision of the Tarim block with the central Tien Shan, a continental fragment still separated from the Asian landmass by at least one paleo-ocean (Allen et al. 1993; Carroll et al. 1995). Some 70 m.yr. later, the northern Tien Shan island arc was accreted to the northern margin of the combined Tarim–central Tien Shan continental block (inset, fig. 1), effectively closing the paleo-ocean basin. By the Early Permian, Central Asia was fully amalgamated (Burtman 1975; Windley et al. 1990; Avouac et al. 1993), after which time a less active tectonic regime prevailed until the collision of India in the Early Tertiary (~50–55 Ma;

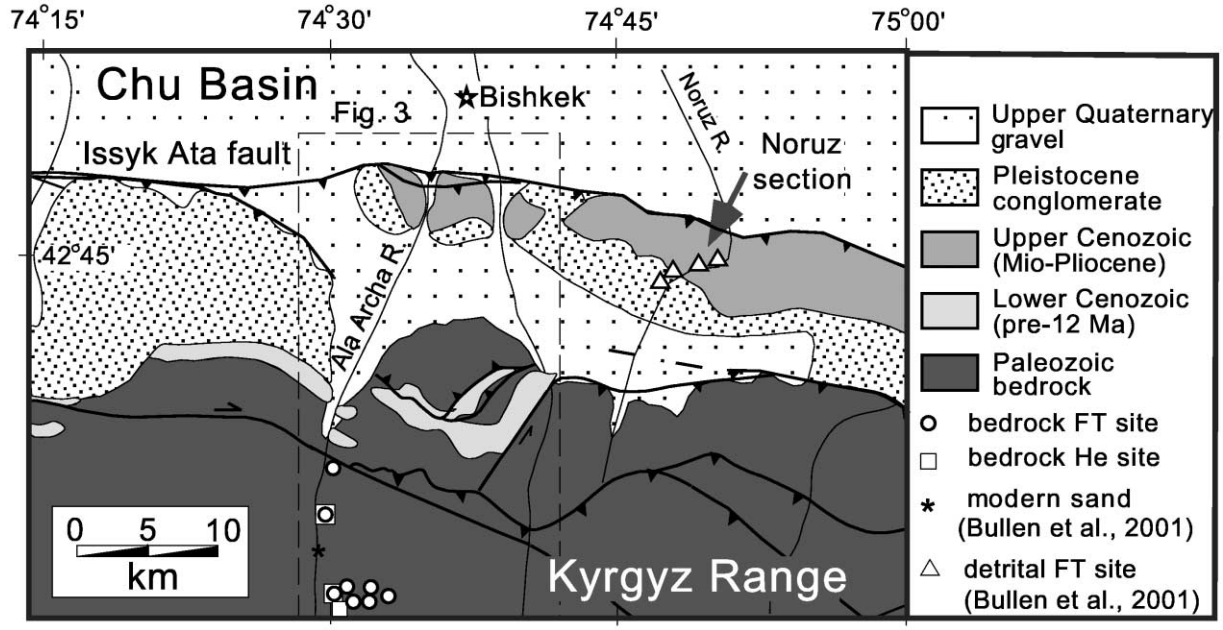

Figure 2. Geologic map of the Chu basin and adjacent Kyrgyz Range (modified after Trofimov et al. 1976 and Mikolaichuk 1999).

Molnar and Tapponier 1975; Patriat and Achache 1984).

An exception to this period of relative quiescence is faulting associated with thick Triassic and Jurassic strata in the Turpan and Junggar basins in the eastern Tien Shan and in the northern Tarim basin (Burtman 1980; Hendrix et al. 1992; Burtman et al. 1996). Coeval deposits in the western Tien Shan are restricted to isolated accumulations along the flanks of a few intermontane basins, where paleogeographic reconstructions depict clastic input from the northern Tien Shan into intermontane basins in the central and southern portions of the range (Atlas Kyrgyzskoi 1987). We infer from these reconstructions that the northern Tien Shan experienced a modest amount of exhumation in Jurassic time, an event that left a discernible thermochronologic imprint.

The Tien Shan remained quiescent for the remainder of the Mesozoic and much of the Cenozoic, including some 20–40 m.yr. after the collision of India in the Early Eocene. This long period of stability resulted in the beveling of topography and a creation of a regionally extensive, low-relief unconformity (Norin 1941; Burtman 1975; Bally et al. 1986) that now functions as a useful marker for tracking structural deformation (Cobbold et al. 1996). Up to 5 km of upper Cenozoic strata accumulated above this unconformity in the Kyrgyz Tien Shan since the Middle Miocene (Chediya et al. 1973). The parallelism of the overlying Cenozoic strata with the unconformity surface attest to the absence of folding of the unconformity before deposition of these strata.

During the past 150 yr, the Tien Shan has been the site of several of the world's largest earthquakes ($M > 8$; Molnar and Deng 1984; Ghose et al. 1997). Aftershock sequences suggest that such faults extend through the upper crust to depths of 15–20 km along planar faults with steep (~45°–50°), uniform dips (Ghose et al. 1997). Although many of these active structures are located at the margins of east-west-trending intermontane basins, a considerable component of strain is also accommodated by younger and more active fault systems that have recently propagated into the former depositional basins (fig. 2).

Methods

Thermochronologic data collected from transects with significant topographic relief have successfully been used to define rates of exhumation and the initiation of rock uplift events (e.g., Fitzgerald et al. 1995; Stockli et al. 2000). Many of these studies use fission track dating and rely on the identification of an exhumed apatite partial annealing zone (PAZ). The fluorapatite PAZ is an idealized

thermal zone between ~60° and 110°C in which fission tracks progressively shorten. At temperatures <60°C, tracks effectively do not shorten, whereas at temperatures above ~110°C, tracks anneal rapidly (Green et al. 1989). Periods of slow cooling followed by rapid cooling preserve a break in slope in an age versus elevation plot that is characteristic of the base of a PAZ (Fitzgerald et al. 1995; Stockli et al. 2000). As this relict PAZ is progressively exhumed through surface erosion, a new PAZ migrates downward with respect to the rock column. The age of the preserved break in slope is commonly inferred to date the onset of rapid exhumation and cooling because of rock uplift. To capture the cooling history of the northern Tien Shan, eight bedrock samples were collected from a granitic pluton that crystallized during the Ordovician (Atlas Kyrgyzskoi 1987) and is at present exposed in the Ala Archa catchment on the north flank of the Kyrgyz Range (figs. 3, 4). The six higher samples constitute a steep 1500-m-high relief section spanning a horizontal distance of ~3 km (fig. 4). The two lowest samples lie along the Ala Archa River Valley and are closer to the range front. All together, the eight sites span 2.4 km of vertical relief.

The boundaries of the apatite PAZ are not always well defined because variations in apatite composition can affect the annealing behavior of tracks in an individual crystal (Green et al. 1985; Crowley et al. 1990; Carlson et al. 1999). Although far less common than Fl-rich apatites, Cl-rich apatites have been shown to retain tracks at ~150°C (Carlson et al. 1999). The partial annealing zone (Cl-PAZ) for such a composition would range from ~100° to 150°C and, hence, would occupy a deeper level in the crust than would a typical fluorapatite PAZ (F-PAZ). There are a number of ways that apatite composition is determined, but the most common is to use an electron microprobe on individual grains. A newly developed technique involves the measurement of etch pit diameters, where Cl-rich grains (>2 weight % chlorine) have etch pit diameters greater than ~1.75 μm, and Fl-rich grains typically have etch pit diameters <1.75 μm (Carlson et al. 1999; R. A. Donelick, pers. comm.). Mean etch pit diameters and electron microprobe measurements were recorded for five of the eight samples collected from the vertical transect (fig. 6; table 1).

U-Th/He dating of apatite has recently emerged as a robust low-temperature dating technique. Similar to the PAZ in the fission track system, a zone of helium partial retention (PRZ) exists between ~40° and ~80°C (Wolf et al. 1998; Stockli et al. 2000). At temperatures less than ~40°C, He is fully retained in apatite, whereas at temperatures greater than ~80°C, He completely diffuses from the crystal lattice. With a typical continental geotherm (20°–30°C/km), the base of the helium retention zone is located at ~2.5–4 km depth, ~1 km above the base of an idealized F-PAZ. The effective closure temperature for the U-Th/He system depends

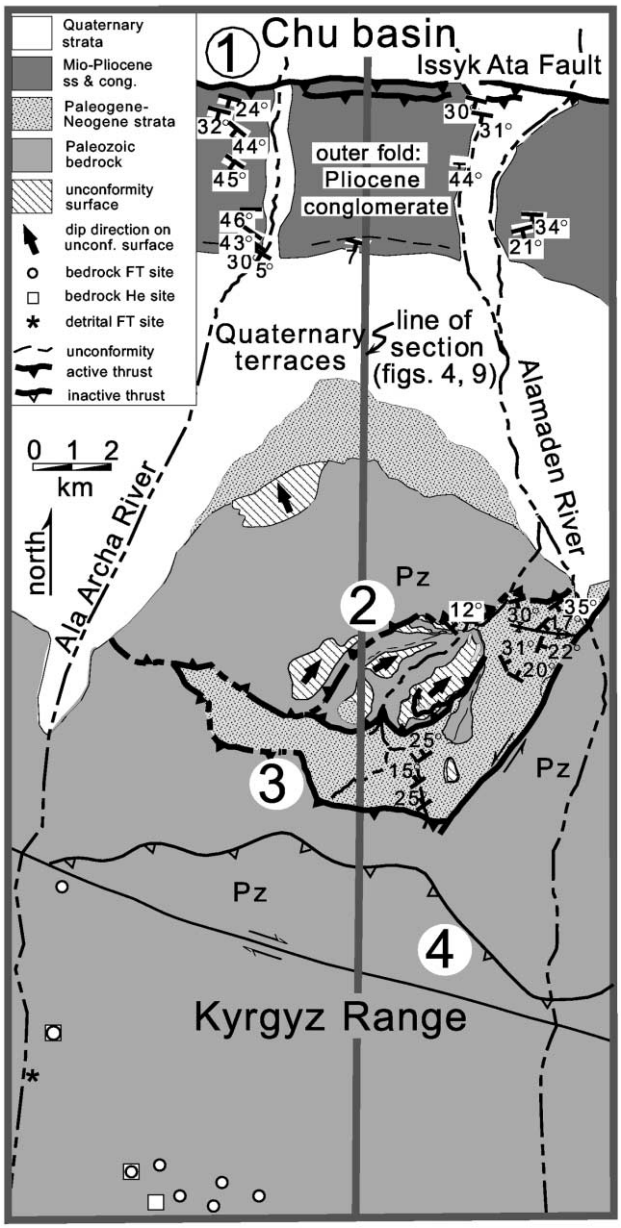

Figure 3. Simplified structural map of central Kyrgyz Range and Chu basin. The following structural zones are highlighted: *1*, north-vergent foreland basin thrusts; *2*, south-vergent backthrusts with Paleozoic rocks in their hanging walls; *3*, north-vergent bedrock thrusts; and *4*, strike-slip faults. See figure 1 for location.

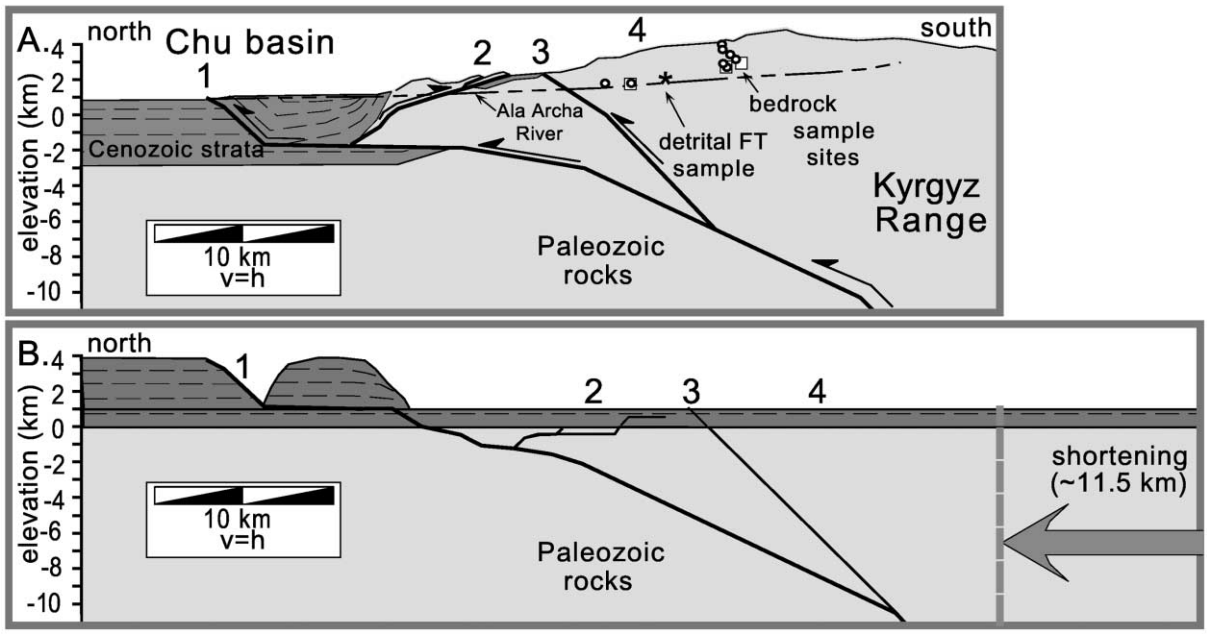

Figure 4. *A*, Structural cross section of the Kyrgyz Range and southern Chu basin showing fission track sample sites. Dashed line within the Kyrgyz Range depicts the approximate valley bottom of the Ala Archa River. Faults are numbered as in figure 3 (*1*, Issyk Ata Fault; *2*, backthrusts; *3*, forethrust of Paleozoic over Cenozoic; *4*, pre-Cenozoic faults within Paleozoic rocks). *B*, Restored, balanced section. Fault numbers are the same as above. By analogy with many other Kyrgyz thrust faults involving Paleozoic rocks, folding of the Paleozoic occurs during fault propagation toward the surface. The presence of older Cenozoic strata across the range to the south of fault 3 is speculative.

on both apatite grain size and the rate of cooling (Wolf et al. 1998; Farley 2000). Larger grains and more rapid cooling are characterized by higher closure temperatures. For the grain sizes and typical cooling rates of this study, we use a closure temperature of 70°C (Farley 2000). U-Th/He cooling ages were determined for those samples in our vertical traverse that yielded sufficiently large and inclusion-free apatite crystals (table 2).

In mountain belts with relatively simple deformational histories, a vertical "stratigraphy" of bedrock cooling ages can exist (Stock and Montgomery 1996). Catchments incised into these mountains reveal a suite of ages that is a function of the depth of erosion into what is essentially a layer cake of cooling ages. If the vertical age distribution is known, then a succession of samples collected from a nearby basin can reveal changes in the frequency of detrital mineral cooling ages through time and provide insights on the history of incision into the source area (Garver et al. 1999; Bernet et al. 2001). In this study, we compare our bedrock fission track ages with the single-crystal fission track ages from detrital apatite grains (Bullen et al. 2001) extracted from both upper Miocene sandstones and modern river sediment in the foreland basin bounding the Kyrgyz Range. The ages at each site were decomposed into the minimum number of significant components using a binomial peak-fitting routine (Galbraith and Green 1990; Bullen et al. 2001). Comparisons of ages of the youngest component peak with those revealed by our vertical relief transect permit limits to be placed on the magnitude and timing of incision of the Kyrgyz Range over the past 20 m.yr.

Whereas thermochronologic studies can define a cooling history, they rarely reveal how much shortening occurred along a particular structure at any given time. In order to define the sequence, magnitude, and rates of shortening, we have mapped a 30-km-long swath from the central Kyrgyz Range to the adjacent foreland and constructed a balanced cross section along this transect. We subsequently use data on the age of faulting and the cooling/erosion history to define a deformation history. Finally, we combine analysis of a 90-m digital elevation model with reconstructed changes in crustal thickness and shortening estimates to assess the compatibility of these independent estimates.

Table 1. Bedrock Fission Track Results from the Kyrgyz Range, Northern Tien Shan

Sample	Elevation (km)	Number of grains	Spontaneous track density ($\times 10^5$ cm^{-2})	Induced track density ($\times 10^5$ cm^{-2})	χ^2 probability	Fission track age (Ma)	Uranium content (ppm)	Mean track length (μm)	Etch pit diameter (μm)	Mean Fl/Cl
212-12	3.97	10	1.94 (16)	1.66 (137)	16.5	20.3 ± 5.5	19.9	…	…	143.88
212-13	3.63	16	5.73 (177)	9.72 (300)	49.9	103.2 ± 11.3	11.5	11.02 ± 2.61 (136)	1.74 (136)	.56
212-8	3.4	19	2.33 (64)	2.40 (659)	58.2	15.9 ± 2.2	30.5	…	1.12 (5)	81.1
212-9	3.20	20	3.39 (102)	3.82 (1150)	5.6	14.7 ± 1.7	48.1	12.07 ± 1.58 (30)	1.18 (30)	71.24
98-30	2.80	19	9.03×10^{-4} (28)	1.31 (407)	45.4	10.5 ± 2.1	17.9	…	…	…
212-14	2.69	20	3.65 (102)	5.63 (1575)	5.8	11.5 ± 1.3	66.1	12.79 ± 1.82 (126)	1.50 (126)	7.41
212-16[a]	2.24	29	1.79 (56)	2.08 (650)	0	15.6 ± 2.3 **12.0 ± 2.8 (F)** **46.9 ± 27.0 (Cl)**	23.9	12.92 ± 1.98 (61)	1.37 (61)	5.32
98-33	1.80	8	1.27 (18)	1.85 (260)	31.3	10.8 ± 2.7	24.8	…	…	…

Note. Ages recorded are pooled ages using all grains, with error reported at 1σ level. Mean ζ of 104.83 was calculated for us from seven analyses of standards (Durango and Fish Canyon Tuff). Numbers in parentheses are sample sizes.
[a] Component age populations for sample 212-16, shown in bold, were defined by statistical methods of Galbraith and Green (1990).

Results

Structural Mapping and Fault Displacements. Structural, stratigraphic, and geophysical data from a transect spanning the Kyrgyz Range and the Chu basin (fig. 3) serve to delineate the geometry and magnitude of Cenozoic shortening. We identify four zones of Late Cenozoic faulting (fig. 3), each characterized by a different style of deformation. From north to south, these include (1) north-vergent thrusts that cut the foreland-basin fill and expose upper Cenozoic foreland strata, (2) south-vergent backthrusts that either imbricate Paleozoic rocks or place them over upper Tertiary strata, (3) north-vergent thrusts that carry Paleozoic rocks over these same upper Tertiary strata, and (4) thrust and strike-slip faults in Paleozoic rocks that are considered to have minimal Cenozoic displacement (fig. 3).

Well logs and seismic data from the Chu basin indicate a total of ~5 km of Cenozoic strata in the Chu basin in the region of our transect (Chediya et al. 1973). These strata are cut by the Issyk Ata Fault, which dips to the south at 30°–45° and overthrusts upper Quaternary gravels. Late Quaternary fluvial terraces along the Alamaden and Ala Archa Rivers (fig. 3) display fault scarps >30 m high, attesting to the recent displacement along this fault. Hanging-wall strata dip parallel to the fault, steepen from ~25°–30° near the emergent fault surface to ~40°–45° through most of the hanging wall, and, overall, define an ~40° dip panel ~3 km thick. The hanging wall consists of tan and pink fluvial sandstone and siltstone that resemble Mio-Pliocene strata (Chu Formation; Chediya et al. 1973) that are widely preserved in the Tien Shan. These are overlain by Plio-Pleistocene conglomerates with decreasing dips in their uppermost exposures. These dip changes are typical of syntectonic conglomerates (Anadón et al. 1986) and suggest that deformation began during their deposition. The position of the axial surface that defines the ramp-flat transition is indicated by folding of Quaternary terraces (Thompson et al. 2002) as they are translated through this surface and by abrupt decreases in the dip of the youngest strata in the hanging wall. Given that the hanging-wall cutoff is not preserved along the Issyk Ata Fault, the minimum shortening is ~4.5 km (fig. 4) on the basis of fault dips of 45° (Ala Archa Valley) and 35° (Alamaden Valley).

Backthrusts juxtapose Paleozoic metavolcanic and plutonic rocks with Cenozoic clastic strata (Mikolaichuk 1999) ~15 km south of the Issyk Ata Fault (figs. 3, 4). These gypsiferous and highly oxidized Cenozoic strata contrast markedly with the tan and pink fluvial strata exposed to the north in the hanging wall of the Issyk Ata Fault and suggest that either there are abrupt facies variations across this 15-km distance or the overthrust strata predate those preserved in the Issyk Ata hanging wall. We prefer the latter interpretation because these overthrust strata closely resemble the basal Cenozoic

Table 2. U-Th/He Results from the Kyrgyz Range, Northern Tien Shan

Sample	Elevation (km)	Number of grains	Raw age (Ma)	Standard deviation (Ma)	Fission track factor	Corrected age (Ma)	Standard deviation (μm)	Uranium content (μm)	Thorium content	He (ncc/mg)
212-10	2.935	7	5.90	.45	.58	10.16	.77	25.5	39.0	26.2
212-14	2.690	13	4.06	.07	.64	6.35	.11	39.0	80.5	29.6
212-16	2.240	9	2.06	.17	.68	3.03	.24	12.1	31.0	5.7

Note. Ages reported at 1σ level. Age correction is based on methods described by Farley et al. (1996).

strata (Kakturpak and Shamsi Formations; Chediya et al. 1973) that are commonly preserved in the Kyrgyz Tien Shan. The extensive unconformity surface that regionally truncates the Paleozoic rocks is well preserved within several of the thrust slices (hachure, fig. 3). The contact with the overlying Cenozoic strata is readily traced, and broad areas (several square kilometers) of the nearly undissected unconformity surface create elongate dip slopes. Given the initial, near horizontal attitude of the unconformity surface in mid-Cenozoic time (Chediya et al. 1973), its present extent and orientation define two major imbricate, low-angle thrust sheets. These are further imbricated by small-displacement (10s–100s of meters) thrust faults. Again, no hanging-wall cutoffs are preserved, such that the observed magnitude of shortening on the backthrusts of ~4 km is a minimum (figs. 3, 4).

South 2 km from the leading edge of the backthrusts, these older Cenozoic strata are overthrust by an ~30°-dipping, north-vergent fault carrying Paleozoic rocks in its hanging wall over Cenozoic clastic strata (figs. 3, 4). The Cenozoic strata in the footwall can be traced through several folds between the backthrusts and this forethrust. In several places, the thrust fault is well exposed, revealing its clear southward dip and truncation of folded Tertiary strata, including conglomerates lithologically analogous to the commonly occurring, basal Cenozoic strata found elsewhere in the Tien Shan (Chediya et al. 1973). Although it is well preserved in the backthrust sheets, the unconformity surface that is regionally bevelled across the Paleozoic rocks is not preserved in the hanging wall, so there is no direct measure of the magnitude of offset on this fault. Shortening must be >0.5 km (the thickness of the Cenozoic strata in the footwall; fig. 4) and is likely to be ~2–3 km. The map pattern suggests that the most southerly exposed Cenozoic strata could represent a window beneath a single folded thrust sheet (fig. 3). This interpretation is, however, considered unlikely because, as shown by field observations, the more northerly thrusts (our backthrusts) would have had to propagate downward to the north through both Cenozoic and Paleozoic rocks.

Although there are numerous faults within the Paleozoic rocks of the Kyrgyz Range (Mikolaichuk 1999), we have not been able to establish Cenozoic offsets on most of these faults (fault 4; fig. 3) and consider them to have been largely inactive during Cenozoic times. The oblique, sinistral strike-slip fault in the east half of the study area truncates thrust 3 (fig. 3), and geodetic studies suggest that this fault may be slipping at ~1 km/m.yr. (Abdrakhmatov et al. 1997). If correct, this would require additional, presently undetected slip on fault 3 (fig. 3) or on faults within the Paleozoic rocks along our transect.

In the absence of hanging-wall cutoffs, our displacement estimates must be considered as minimums. The cumulative displacement is 10–12 km: 4.5 km on the Issyk Ata Fault, 4 km on the backthrusts, and 2–3 km on the southerly (Paleozoic-over-Cenozoic) thrust fault (fig. 4).

Bedrock Thermochronology: Apatite Fission Track Dating. Eight bedrock samples yielded interpretable fission track ages, ranging from 103 ± 11 to 10.5 ± 2.1 Ma, which generally increase with elevation (all ages ±1σ; fig. 5; table 1). The apatite fission track age versus elevation profile from the Kyrgyz Range contains a distinct break in slope at 11 Ma and ~2.8 km elevation (fig. 5), which we interpret as representing the base of an exhumed Fl- (Fitzgerald et al. 1995; Stockli et al. 2000). The ~1-km-thick section below 2.8 km exhibits a narrow range of fission track ages (10.5–11.5 Ma), indicating rapid cooling and exhumation at that time. Given the uncertainties in fission track ages, it is difficult to assign a representative exhumation rate for this interval. However, the break in slope at 11 Ma and accompanying U-Th/He age data justify rates on the order of 1.0–1.5 km/m.yr.

Both etch pit measurements (1.74 μm) and electron microprobe analyses (Fl/Cl = 0.56) indicate that the sample at an elevation of 3.6 km, which yields an old age of 103 ± 11 Ma, is Cl rich (fig. 6; table 1). Given the higher annealing temperature of Cl-rich apatites (150°C), the implications of this old fission track age are striking: temperatures since ~100 Ma have remained below 150°C (Carlson et al. 1999). Until ~10 Ma, this sample had cooled

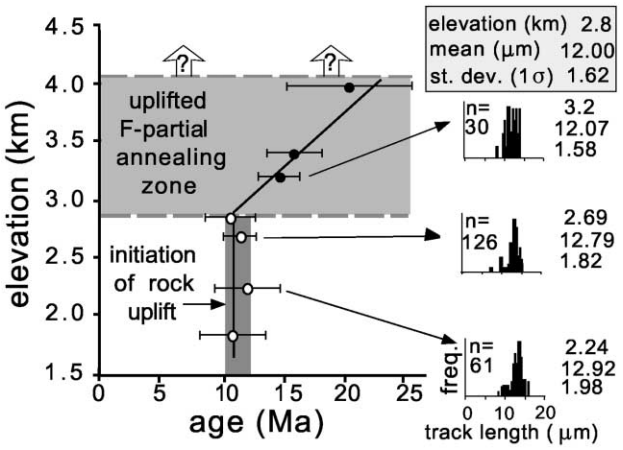

Figure 5. Bedrock apatite fission track ages from the central Kyrgyz Range. Track-length (TL) data (*right side*) give number of counted TLs (*n*), elevation, mean TL, and standard deviation of the TL distribution. The break in slope at ~2.8 km defines the base of the partial annealing zone (PAZ; 110°C) for F-apatite and delineates the initiation of rapid exhumation at ~11 Ma. Shortened track lengths and large standard deviations for sites above 2.800 km indicate these sites remained within the PAZ after 10 Ma.

only ~60°C, yielding a cooling rate of <1°C/m.yr. over this 90-m.yr.-long interval. Therefore, we infer that the northern Tien Shan experienced tectonic quiescence for the majority of the Cenozoic and the Late Cretaceous.

By analogy with the Cl-rich sample noted above, we interpret the spread in grain ages from the sample at a 2.24-km altitude to result from a mixture of chlorapatite and fluorapatite crystals. This sample was collected from the same granitic pluton as the other samples, yet it is the only one that fails the χ^2 test (<5%; Green 1981), indicating that the observed grain ages do not belong to a single population. The data show two grain-age populations of 46.9 ± 27 and 12.0 ± 2.8 Ma, which we attribute to the cooling of fluorapatite and chlorapatite, respectively (see Brandon et al. 1998). F/Cl ratios from this sample are intermediate between those of the chlorapatite sample at 3.6 km and those of the F-apatite sites (fig. 6*B*). Therefore, the old sample at 3.6 km (103 ± 11 Ma) and old population of grain ages at 2.24 km (46.9 ± 29 Ma) are effectively higher temperature thermochronometers that record this very slow exhumation in the Late Cretaceous and Tertiary.

Although mean track lengths increase at lower elevations (fig. 4), mean lengths increase to only 12.9 μm and display relatively large standard deviations. Such shortened tracks and broad track-length distributions are characteristic of slow exhumation rates and significant time in the partial annealing zone (Gleadow et al. 1986). Therefore, rocks below 2.8 km elevation must have remained at elevated temperatures (>70°C) after ~11 Ma, such that they resided within the F-PAZ. If the inferred exhumation rates of ~1 km/m.yr. at ~11 Ma had been sustained until present, we would expect ~11 km of total exhumation and apatite fission track ages of 3–5 m.yr. at the modern surface. However, because fission track ages of >10 m.yr. are present at the surface, exhumation rates must have slowed abruptly after 10–11 Ma.

U-Th/He Dating. Although apatites were extracted for U-Th/He dating from all bedrock samples, only three samples yielded apatites that were deemed to be sufficiently large and inclusion free for dating. Similar to the fission track ages, the U-Th/He dates (table 2) also vary systematically with

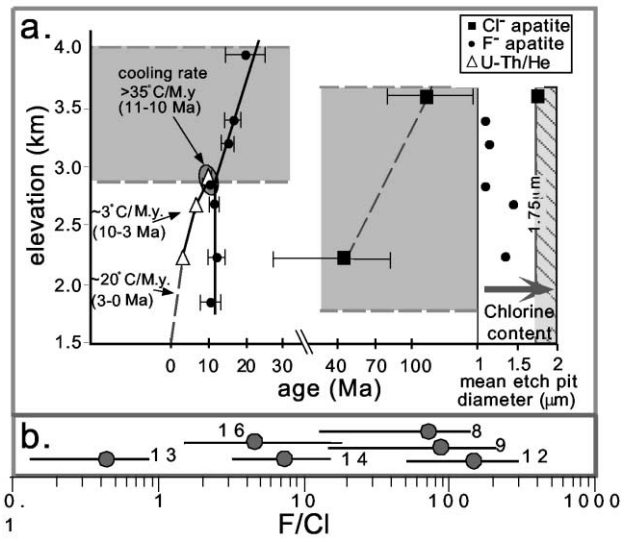

Figure 6. *a*, All age data from the central Kyrgyz Range. Gray rectangles represent inferred partial annealing zones for F-apatite (*left*) and Cl-apatite (*center*). Hachured zone (*right*) represents range of expected etch pit diameters for Cl-apatites. Cl-apatite fission track samples at 3.36 km (103 Ma; sample 13) and in a mixed-age sample at 2.24 km (49 Ma; sample 16) span 1.5 km and are interpreted to define much of a Cl-PAZ. U-Th/He ages and fission track ages (enclosed by dark ellipse) at ~2.8 km indicate rapid cooling between 10 and 11 Ma. Cooling rates are lower from 10 to 3 Ma (gentle age-elevation gradient) and accelerate after 3 Ma to >20°C/m.yr. *b*, F/Cl ratios for selected bedrock fission track samples clearly depict the chlorapatite-rich sample (13) and the sample with a mix of fluorapatite and chlorapatite (16).

elevation, ranging from 10.2 ± 0.8 to 3.0 ± 0.2 Ma (fig. 6). The He age of 10.2 ± 0.8 Ma is indistinguishable from the apatite fission track age of 10.5 ± 2.1 Ma collected 135 m below the He site. This similarity implies that rocks at ~2.8 km cooled rapidly from ~110° to ~75°C (Wolf et al. 1998) in ~1 m.yr.

Conversely, the presence of significantly younger (7 and 3 Ma) He ages below 2.8 km indicates that the rapid cooling slowed around 10 Ma; otherwise, these sites should have ages more similar to the fission track data. These He ages support evidence from the shortened fission track lengths (fig. 3), indicating that rocks below 2.8 km remained at elevated temperatures after 10 Ma. Following ~7 m.yr. of slow cooling (~3°C/m.yr.), cooling rates accelerated after 3 Ma to >20°C/m.yr., on the basis of the 3.0 ± 0.2 Ma He age.

Interpretation of the Thermochronologic Data. When based on thermochronology, reconstruction of exhumation in the Kyrgyz Range requires assumptions concerning the past geothermal gradient. The modern geothermal gradient in this area is ~26°C/km (Shvartzman 1992), which lies within the expected range of continental geotherms. We assume that the gradient has been similar since 11 Ma. Although we recognize that the geothermal gradient will change in response to accelerated erosion and topographic relief (Stüwe et al. 1994; Mancktelow and Grasemann 1997), the generally modest and short-lived rates of erosion interpreted here suggest that the geothermal gradient would not be strongly perturbed. The modern geothermal gradient is, therefore, used to estimate the paleodepth as well as the magnitude and rate of exhumation of various samples. For example, the base of the F-PAZ at 11 Ma would be expected to be ~4 km beneath the surface. The vertical separation between the 3-Ma and 10-Ma He samples (~0.7 km; fig. 6) implies exhumation rates of 0.1 km/m.yr. during this interval. Similarly, the vertical separation of the ~11-Ma fission track samples (1 km; fig. 5) and the juxtaposition of the 10-Ma He date (2.935 km; fig. 6) with the 11-Ma fission track age (2.8 km; fig. 6) imply rapid exhumation (~1.5 km/m.yr.) at that time. The youngest He sample cooled to surface temperatures (~10°C) in 3 m.yr., implying a mean exhumation rate of ~0.7–0.8 km/m.yr. The chlorapatite sample at 3.6 km (fig. 6) indicates very slow cooling (<1°C/m.yr.) between 11 and 100 Ma, equivalent to an average exhumation rate of <0.05 km/m.yr. Such rates are equivalent to the rates of lowering measured at 10^5–10^6-yr time scales on low-relief bare bedrock surfaces (Bierman 1994; Small et al. 1997) and are consistent with the Early Cenozoic development of the regional unconformity surface in the Kyrgyz Range and the absence of pre-Miocene folding.

In sum, as interpreted from these age data, the exhumation history of the Kyrgyz Range can be divided into four discrete periods (fig. 7): (1) tectonic quiescence prevailed from 103 to 11 Ma (exhumation rates <0.05 km/m.yr.); (2) rapid exhumation began at ~11 Ma (1.0–1.5 km/m.yr.); (3) exhumation rates decreased between 3 and 10 Ma (0.1–0.3 km/m.yr.); and (4) exhumation rates accelerated after

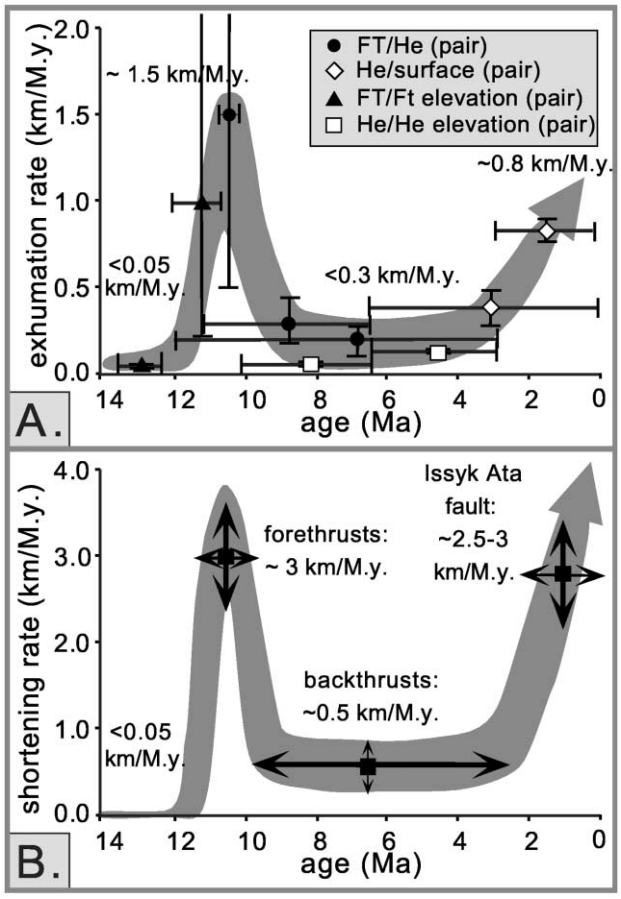

Figure 7. Exhumation (*A*) and shortening (*B*) rates from 14 Ma to present reconstructed from both thermochronologic data and field mapping. Horizontal arrows represent the duration of the calculated exhumation and shortening rates. Calculations are based on these assumptions: fission track (*FT*) closure temperature = 110°C; He closure temperature = 70°C; surface temperature = 10°C. Rates based on elevation differences are defined by Δ height/Δ age. Rates based on temperature differences are first converted to height differences based on the assumed geothermal gradient (26°C/km). Estimates of exhumation rate error were calculated from age uncertainties (1σ).

~3 Ma (0.8 km/m.yr.). If changes in cooling rate reflect pulses in tectonic activity, then mountain building along the northern Tien Shan was highly variable.

Detrital Mineral Dating. Additional insights on the exhumation and deformation history can be gleaned from study of fission track ages of detrital apatite from synorogenic strata (Bullen et al. 2001). In this study, samples were collected from both the modern Ala Archa River (figs. 2, 8), which drains the rocks sampled by our bedrock fission track transect, and the Miocene to Pleistocene strata carried in the hanging wall of the Issyk Ata thrust fault (fig. 2; Bullen et al. 2001). The modern Ala Archa sample (fig. 8) comprises two grain-age populations with mean ages of ~17 and ~78 Ma. Given the uncertainties of the data, the young component population is consistent with the bedrock cooling ages that we sampled in the Ala Archa catchment (fig. 5) and indicates that these Miocene bedrock cooling ages are well represented in the bedload of the modern rivers. The older population indicates that either higher parts of the catchment or (more likely) the more hinterlandward parts of the catchment have experienced substantially less exhumation than is experienced in the vicinity of our vertical relief transect. These areas would provide the older ages that are not observed in our bedrock samples.

A magnetostratigraphically dated section (Bullen et al. 2001), located ~20 km east of our bedrock transect (fig. 2), comprises analogous upper Cenozoic strata in the Issyk Ata hanging wall and provides a temporal context for four additional detrital samples. Two older samples were collected from strata dated at 8.5 and 4.5 Ma (fig. 8), while two younger samples were retrieved from an overlying 1-km-thick conglomerate succession with an estimated age between ~1 and ~3 Ma (see Bullen et al. 2001). Analysis of these detrital data yields striking

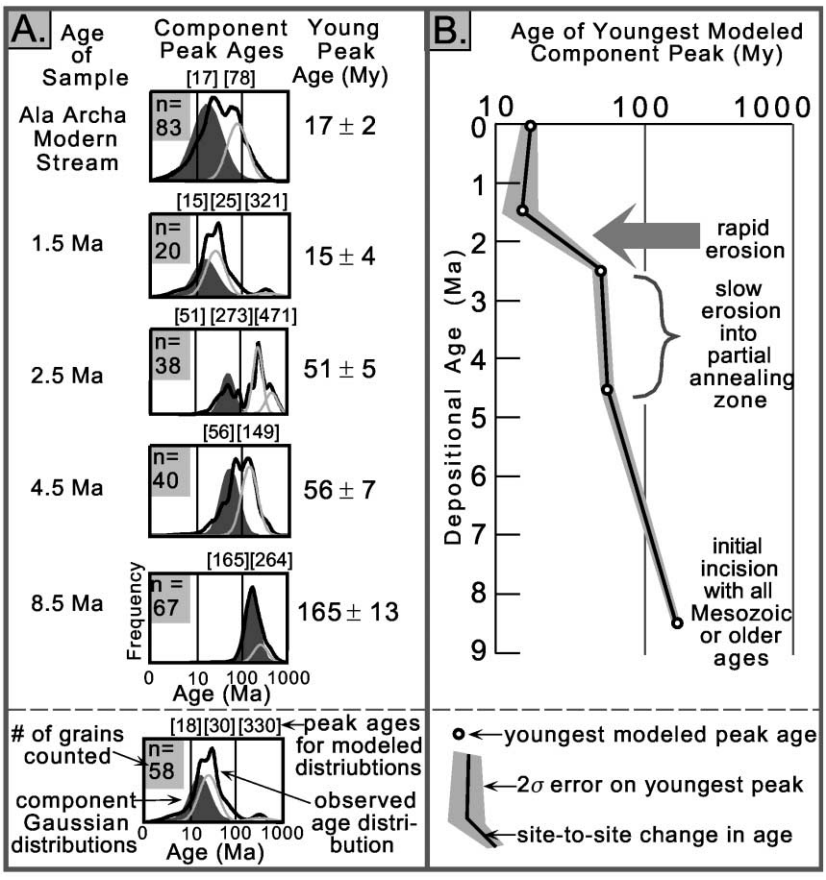

Figure 8. Detrital fission track data from the Noruz magnetostratigraphic section and Ala Archa modern river (our fig. 2; Bullen et al. 2001). Grain-age populations, or peaks, were statistically separated using the binomial peak-fitting routine of Brandon (1996). Youngest peaks (*shaded gray*) decrease in age up-section from 165 to 15 Ma and document variations in the rate of erosional exhumation into the apatite partial annealing zone.

insights into the erosion history of the Kyrgyz Range (fig. 8). Approximately 2 m.yr. after rapid erosion began, the detrital apatites deposited at 8.5 Ma were still dominated by Mesozoic and older ages. The Jurassic age of the youngest population (165 Ma) is consistent with the age of the last major thermal and erosional event in the Kyrgyz Range. The absence of a younger component population indicates that canyons had not yet incised into the F-PAZ, where Cenozoic cooling ages would be expected. By 4.5 Ma, Early Cenozoic detrital ages define the youngest component peak, indicating incision into the F-PAZ, which would initially have been at depths of ~3–4 km (on the basis of a geothermal gradient of 26°C/km). The absence of dates younger than ~20 Ma suggests that the lower half of this PAZ was not contributing significantly to the sediment load at 4.5 Ma. Interestingly, there is no statistical change in the youngest detrital age population between 2.5 and 4.5 Ma (fig. 8), which suggests that additional incision was minimal during this interval. This conclusion is consistent with the He ages that also indicate much slower incision (~0.1 km/m.yr.; fig. 7) during this interval. There is a striking difference, however, between the young peak ages of the 1.5- and 2.5-Ma samples at the Noruz magnetostratigraphic section (fig. 8). By 1.5 Ma, the detrital record is indistinguishable from the modern sample at Ala Archa, indicating that rivers had incised entirely through the fossil PAZ. The similarity of the 1.5-Ma sample to the modern sample also suggests that the topographic relief of the contributing catchment (Stock and Montgomery 1996) was similar to the present-day Ala Archa catchment.

In sum, the results of the detrital dating corroborate the inferences on changes in the relative rates of exhumation during the past 10 m.yr. During the Late Miocene (<10 Ma), about 2–3 km of incision (into the PAZ) occurred within the Kyrgyz Range. During much of the Pliocene, rates of incision were significantly slower (<1 km in 4 m.yr.), whereas rates accelerated greatly during the past 2 m.yr.

Discussion

Thermochronology. Most of the interpretation of the bedrock thermochronology is based on the "vertical relief" section. In fact, this sequence of samples is spread out across the landscape: the two lowest elevation sites lie up to 7 km north of the other sites. There exists the possibility that undetected tilting about a horizontal axis could greatly affect the apparent position of any site beneath a reference surface (Stockli et al. 2000), such as the bedrock unconformity. We argue that significant tilting is unlikely to have occurred. First, the surface transect along which the southerly sites were collected is oriented parallel to the range and perpendicular to expected tilt directions, given the pattern of faults. Therefore, even if tilting of up to 30° about an axis parallel to the range had occurred, it would have little impact on the interpretation of this southerly sequence of ages. Second, such tilting could have a major impact on the two more northerly sites. The facts, however, that these low-elevation sites reveal the same cooling ages as the two sites in the south that altitudinally overlie them and that they are different in age from the higher sites in the south argue strongly against significant tilting. Similarly, these consistent ages argue against much displacement on the faults within the Paleozoic rocks that separate the two groups of samples (fig. 3).

The bedrock fission track data in our vertical relief section provide an excellent signal of the initiation of deformation in the Kyrgyz Range. The break in slope in the vertical succession of ages (fig. 5) and the uniform ages beneath that kink indicate abrupt bedrock cooling beginning at ~11 Ma. The amount of rock uplift and erosion had to be sufficient to rapidly cool the ~1-km-thick column of rock that displays the 11-Ma ages. These ages are consistent with the inference that deformation in the Kyrgyz Tien Shan began at ~10 Ma (Avouac et al. 1993; Abdrakhmatov et al. 1996). If the initiation of deformation in the southern Tien Shan occurred in the Late Oligocene to Early Miocene (Hendrix et al. 1994; Sobel and Dumitru 1997; Yin et al. 1998), then our data from the northern Kyrgyz Range require that deformation migrated northward across the Tien Shan between 20–25 and 11 Ma.

A second important inference from our thermochronologic data is that deformation in the Kyrgyz Range was episodic from 11 m.yr. to the present. Rates of cooling were variable (fig. 7), and, given that there is no evidence for a local thermal event during this interval, we interpret these cooling rates to indicate temporal variations in exhumation rates in the Kyrgyz Range. Such variations are incompatible with (1) the concept that deformation, once initiated, proceeds at a constant rate and (2) suppositions that geodetically determined rates of shortening can be reliably extrapolated for millions of years. The Kyrgyz Range data do not necessarily contradict the suggestion that the rate of shortening across the entire Tien Shan was sustained since 10 Ma (Abdrakhmatov et al. 1996), but they do require major shifts in the locus and rates

of deformation across the ranges of the Kyrgyz Tien Shan.

Shortening History. In the following, we synthesize structural, chronologic, and stratigraphic data to reconstruct the shortening history for the three structural zones (fig. 3) with major Cenozoic shortening in the Kyrgyz Range and adjacent foreland. Several lines of evidence can be used to detail the deformation of the Issyk Ata Fault as it propagated into the Chu basin. Both in our transect (figs. 3, 4) and in the Noruz section 20 km to the east (Bullen et al. 2001), the hanging wall directly above the thrust comprises ~3 km of upper Cenozoic strata. Only within the conglomerates, the topmost hanging-wall strata, do dips decrease significantly with respect to the uniform dip panel represented by the underlying rocks. We interpret this dip change to represent the initial displacement along the Issyk Ata Fault. The magnetostratigraphic data from Noruz (Bullen et al. 2001) indicate that faulting initiated within the past 3 m.yr., and the He dates from our transect indicate a striking acceleration in exhumation rates within this same time interval. The detrital fission track ages from Noruz permit us to further restrict the timing of fault initiation. Young component-peak ages are nearly identical from strata deposited at 2.5 and 4.5 Ma (fig. 8), reflecting slow exhumation of the Kyrgyz Range during this interval. We suggest that a major change occurred in the depth of incision in the source area between 1.5 and 2.5 Ma. We suspect that this change resulted from enhanced rock uplift in the Kyrgyz Range as displacement began along the Issyk Ata Fault after 2.5 Ma. Given the minimum shortening of 4–5 km on the fault, this initiation age indicates that average shortening rates have been 2–3 km/m.yr. over the past 2.5 m.yr. Such rates are similar to those rates (2–3.5 km/m.yr.) derived from fault trenches along the Issyk Ata Fault (Chediya et al. 1998; Thompson et al. 2002).

The timing of initiation of deformation along the southernmost thrust fault is derived primarily from the bedrock thermochronology. The observation that this fault overrides poorly dated Early Tertiary strata provides a broad limit on the timing of thrusting. However, we interpret the abrupt increase in the rate of cooling recorded by the fission track data at 11 Ma to result from rock uplift, production of topographic relief, and enhanced exhumation as faulting initiated. The amount and rate of shortening required by this exhumation depends on the dip of the fault and the magnitude of rock uplift and related erosion needed to cause the observed cooling. On the basis of both the thermal constraints associated with the He ages and the relatively short fission tracks, the magnitude of exhumation was no more than 2 km. However, a minimum of ~1–1.5 km of exhumation must have occurred, considering the exposed thickness (1 km) of the rock column with uniform cooling ages and the apparent rate of cooling between 10 and 11 Ma (~45°C). At least 2 km of rock uplift must have occurred to drive this magnitude and rate of erosion. We make the assumption that the initial dip of the fault was 45°, which is similar to modern active faults as illuminated by seismicity in the Tien Shan (Ghose et al. 1997). Using a 45° dip, 3 km of displacement along the ramp is required to generate ~2 km of rock uplift. Given that cooling rates abruptly decreased after 10 Ma, we assume that thrusting slowed after this time. If the thrust ramp dipped less steeply, more shortening would be required to achieve the same uplift.

Given the older ages of initial deformation in the southern Tien Shan (Hendrix et al. 1994; Sobel and Dumitru 1997; Yin et al. 1998), it is tempting to suggest that deformation also began earlier in the Kyrgyz Range but is not well expressed in the thermochronology because the dated sections were riding above a very low-angle decollement. We reject this suggestion for the following reasons. First, extensive, low-dip, contractional decollements within highly deformed bedrock are uncommon. Second, the leading edge of the bedrock thrust sheet would have had to extend far to the north or to have experienced extensive erosion. Neither of these is consistent with the structural observations. Finally, neither the detrital nor the bedrock fission track records allow for significant erosion of the hanging wall before 11 Ma.

Although the backthrusts appear to account for at least 4 km of shortening, we have no direct limits on the timing of this faulting (fig. 3). It is likely that these backthrusts exploit the same basement ramp as the range bounding north-vergent thrust (fig. 4), which implicitly places a maximum limit on their initiation (11 Ma). If they were synchronous with propagation of the Issyk Ata Fault, then 8–9 km of shortening occurred in the past ~2 m.yr., which would have caused significantly more cooling than is recorded by the He data. Conversely, if the backthrusts were synchronous with the forethrust in the Paleozoic rocks to the south, they would require 6–7 km of shortening at that time and would necessitate a much gentler ramp angle (10°–12°) through the Paleozoic granites. We consider both of these scenarios to be unlikely. By default, we infer that the backthrusts were active between 3 and 10 Ma, which would correspond to

shortening rates of ~0.5 km/m.yr. Spanning this interval, fission track and He data indicate that rocks above the basement ramp cooled at rates of ~3°C/m.yr., equivalent to only ~0.1 km/m.yr. of exhumation. The structural model most consistent with our field observations and cooling rates involves a new ramp angle of 25° beneath the Kyrgyz Range (fig. 4). If the ramp were steeper, more rock uplift, erosion, and cooling would be predicted than is observed. A less steep ramp angle would be permissible if more shortening was accommodated by the backthrusts.

Paleotopography. By combining the structural and thermal history with the modern topography, we attempt to reconstruct the evolution of the Kyrgyz Range as a topographic feature. Thickness data from drill holes in the nearby Chu basin (Chediya et al. 1973) and from overthrust Cenozoic strata within the Kyrgyz Range indicate that, before the initiation of deformation, the Paleozoic bedrock was buried by 0.5–1 km of Cenozoic strata. If we assume that (1) the surface elevation of these terrestrial strata before 11 Ma was comparable to that of the modern Chu basin (0.5–0.7 km above sea level) and (2) the geothermal gradient was 26°C/km, the base of the F-PAZ partial annealing zone just before uplift would have resided at ~4 km below sea level. Because the base of the exhumed F-PAZ is now at an elevation of ~2.8 km, rocks of the Kyrgyz Range have been uplifted some 6 km since 11 Ma. Given its mean modern elevation of 2.7 km, the central Kyrgyz Range has, if our assumptions hold, experienced ~2 km of surface uplift and ~4–4.5 km of exhumation since 11 Ma (fig. 9).

After the initiation of deformation at 11 Ma, the basin that covered the incipient Kyrgyz Range would have become inverted, building positive topography and therefore driving exhumation. As seen elsewhere in the Tien Shan (Burbank et al. 1999), the weakly lithified Cenozoic strata would have been readily stripped off the uplifting bedrock, thus causing nearly instantaneous exhumation. We interpret that ~2 km of rock uplift and an average of 1.5 km of exhumation resulted in an increase in the mean elevation of 0.5 km at this time (fig. 9*C*). The 4 km of backthrusting is calculated to have caused ~1.5–2 km of rock uplift above a 25° ramp (fig. 9*B*). Given the vertical distribution of bedrock fission track dates and the observed detrital fission track data (fig. 8), we infer that relief increased to ~2.5 km as rivers incised into the uplifted F-PAZ between 4.5 and 8.5 Ma. The observed cooling rates imply that ~0.5–1 km of exhumation occurred during this interval, yielding an increase of ~1 km in the mean elevation. Last, shortening along the Issyk Ata Fault during the past 3 m.yr. caused accelerated rock uplift, cooling, and erosion and created rapid changes in relief and mean elevation (fig. 9*A*).

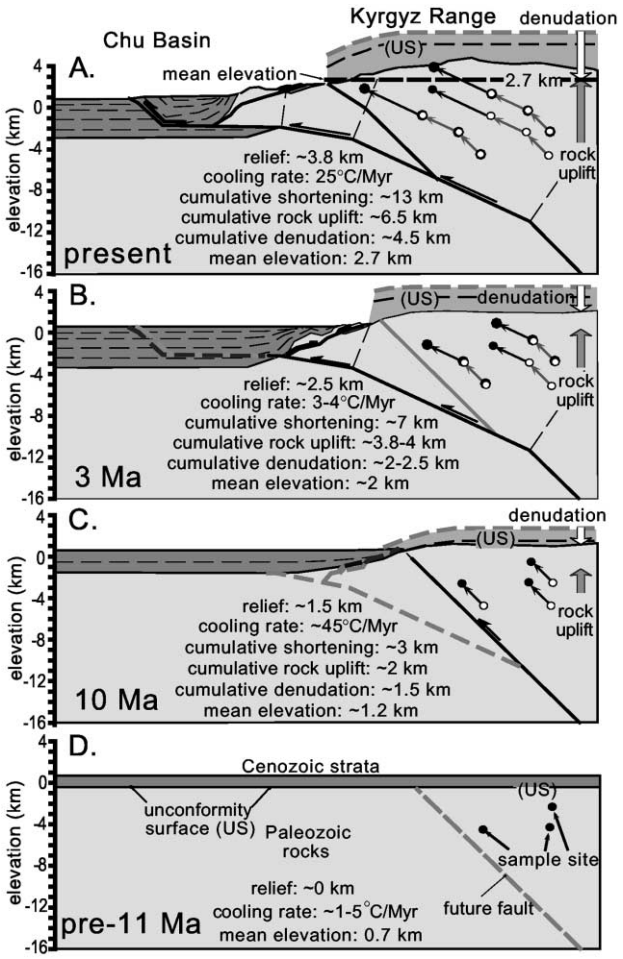

Figure 9. Structure, denudation, surface uplift, and rock uplift for the central Kyrgyz Range. The changing positions of three sample sites are tracked through each step. The geometry of the footwall ramp is constrained from field observations and limits imposed by the thermochronologic data. Four stages are represented: *A*, present-day geometry; *B*, 3 Ma; *C*, 10 Ma; and *D*, before ~11 Ma.

One check of these calculations comes from simple mass balance and isostatic calculations. Our data indicate that a crustal width of ~50 km has been shortened by ~10–12 km, and, on average, 2.5 km of rock has been removed from the area (fig. 9*A*). If we assume that the crust before Miocene deformation had a thickness similar to that of the adjacent Kazakh platform (45 km; Roecker 1999), we can calculate the estimated crustal thickness

and expected change in surface elevation due to shortening and exhumation: 46 km wide × (45 km thick − 2.5 km eroded)/35 km present width = 56 km thickness. The change in crustal thickness of ~11 km would cause ~2 km of surface uplift, assuming local compensation. A change of this magnitude in surface elevation agrees with our reconstructed change in mean elevation (fig. 9). Moreover, the calculated modern crustal thickness beneath the Kyrgyz Range is consistent with the seismically determined variations of crust beneath the Kazakh platform and Kyrgyz Range (Roecker 1999).

Whereas we have interpreted changes in erosion rates as a response to primarily tectonic forcing, others might argue that enhanced erosion could be climatically driven (Molnar and England 1990; Whipple et al. 1999). We suggest that, whereas part of this enhanced incision between 1.5 and 2.5 Ma could be climatically driven, conglomeratic deposition began ~1 m.yr. earlier at ~3 Ma, a time when facies and accumulation-rate changes are observed globally as a response to climate change (Zhang et al. 2001). Enhanced climatically driven erosion would be expected to decrease slope angles and topographic relief while causing relatively minor river incision (Whipple et al. 1999). This is consistent with the similarity of the detrital age distributions at 2.5 and 4.5 Ma (fig. 8) but stands in contrast to the change in detrital ages between 1.5 and 2.5 Ma, which indicate greater relief (Stock and Montgomery 1996) and significantly enhanced incision. Therefore, although we cannot rule out climatically driven erosion, it seems largely overshadowed by the 4–5 km of shortening that occurred along the Issyk Ata Fault and that provided a ready explanation for uplift of the Paleozoic rocks in its hanging wall, increased relief, and deeper incision into rocks lying beneath the uplifted PAZ.

Conclusions

The combination of two different low-temperature thermochronometers with structural mapping, a balanced section, and detrital mineral ages yields details on the timing, rate, and magnitude of deformation and exhumation in the Kyrgyz Range. Not only are the total surface uplift, rock uplift, and exhumation since 11 Ma reasonably well defined (2 km, 6.5 km, and 4.5 km, respectively) but also through comparisons of the thermal, structural, and stratigraphic data, changes during each interval of deformation can be delimited (fig. 9). The most striking result of this synthesis is the highly pulsed deformation of the Kyrgyz Range, as shortening rates varied from ~2–3 km/m.yr. between 10–11 Ma and 0–3 Ma to <0.5 km/m.yr. between 7 and 10 Ma. Such order-of-magnitude variations highlight the inadequacy of extrapolating short-term geodetic rates to geologic time scales, especially when referring to a single mountain range. The apatite fission track and U-Th/He data unambiguously define the initiation of deformation in the Kyrgyz Range as ~11 Ma. For nearly 100 m.yr. before this, cooling rates were <0.5°C/m.yr., implying slow rates of erosion consistent with the development and preservation of a regionally extensive erosion surface bevelled across the pre-Cenozoic bedrock.

These data also provide new insights into the growth of the Tien Shan and evolution of the Indo-Asian collision. If estimates of Early Miocene initiation in the south (Sobel and Dumitru 1997; Yin et al. 1998) and east (Hendrix et al. 1994) are correct, then deformation has migrated from south to north and perhaps from east to west. Given modern shortening rates of ~20 km/m.yr. and an estimated total shortening across the range of 100 km, Early and Middle Miocene shortening must have occurred at considerably slower rates than those at present. The rates of Late Miocene to Quaternary shortening documented in this study for the Kyrgyz Range vary markedly through time and, even at their fastest, represent only a small percentage (<10%–15%) of the geodetic shortening rate across the Tien Shan (Abdrakhmatov et al. 1996). This suggests that, since 11 Ma, deformation has been partitioned among multiple active structures, an inference consistent with the pattern of modern seismicity (Roecker et al. 1993) and faulting (Thompson et al. 2002) in the Tien Shan. Finally, any causal relationship between uplift of the Tibetan Plateau and development of the Tien Shan (Molnar et al. 1993) remains unclear. Whereas Kyrgyz Range development could be approximately synchronous with the inferred maximum uplift of Tibet, the observation that spatial variations in the initiation of the Tien Shan deformation span 10 m.yr. weakens any causal linkage.

ACKNOWLEDGMENTS

We thank the Continental Dynamics Tien Shan team for logistical and research support and J. Lave, K. Abdrakhmatov, and A. Mikoliachuk for field assistance, advice, and provocative discussions. We also thank I. Brewer for critically reviewing the manuscript. R. Donelick and K. Farley provided in-

valuable assistance and advice with the fission track and U-Th/He dating and data analysis. We thank D. Pierce for the microprobe analyses. This work was supported by grants from National Science Foundation Division of Earth Sciences (96-14765), National Aeronautics and Space Administration (NAG-7646), and a fellowship from Anadarko Petroleum.

REFERENCES CITED

Abdrakhmatov, K. Y.; Aldazhanov, S. A.; Hager, B. H.; Hamburger, M. W.; Herring, T. A.; Kalabaev, K. B.; Makarov, V. I.; et al. 1996. Relatively recent construction of the Tien Shan inferred from GPS measurements of present-day crustal deformation rates. Nature 384:450–453.

Abdrakhmatov, K. Y.; Lesek, O. M.; and Kalmeti, Z. A. 1997. About the kinematics of the Alamaden fault. Echo of Science (Izv. Nat. Acad. Sci. Kyrgyz Republic) 1:9–12.

Abdrakhmatov, K. E.; Weldon, R.; Thompson, S.; Burbank, D.; Rubin, C.; Miller, M.; and Molnar, P. 2001. Origin, direction, and rate of modern compression in the central Tien Shan, Kyrgyzstan. Russ. Geol. Geophys. 42:1585–1609.

Allen, M. B.; Windley, B. F.; and Zhang, C. 1993. Palaeozoic collisional tectonics and magmatism of the Chinese Tian Shan, Central Asia. Tectonophysics 220: 89–115.

Anadón, P.; Cabrera, L.; Colombo, F.; Marzo, M.; and Riba, O. 1986. Syntectonic intraformational unconformities in alluvial fan deposits, eastern Ebro basin margins (NE Spain). *In* Allen, P. A., and Homewood, P., eds. Foreland basins. Int. Assoc. Sedimentologists Spec. Publ. 8. Oxford, Blackwell Scientific, p. 259–271.

Atlas Kyrgyzskoi. 1987. Atlas Kyrgyzskoi (vol. 1). Moscow, Academia Nauk Kyrgyzskoi CCP, p. 1–157.

Avouac, J. P.; Tapponnier, P.; Bai, M.; You, H.; and Wang, G. 1993. Active thrusting and folding along the northern Tien Shan and Late Cenozoic rotation of the Tarim relative to Dzungaria and Kazakhstan. J. Geophys. Res. 98:6755–6804.

Bally, A. W.; Chou, I. M.; Clayton, R.; Heugster, H. P.; Kidwell, S.; Meckel, L. D.; Ryder, R. T.; et al. 1986. Notes on sedimentary basins in China. Report of the American Sedimentary Basins Delegate to the People's Republic of China, August 17–September 8, 1985. U.S. Geol. Surv. Open File Rep. 86-327, 108 p.

Bernet, M.; Zattin, M.; Garver, J. I.; Brandon, M. T.; and Vance, J. A. 2001. Steady state exhumation of the European Alps. Geology 29:35–38.

Bierman, P. R. 1994. Using in situ produced cosmogenic isotopes to estimate rates of landscape evolution: a review from the geomorphic perspective. J. Geophys. Res. 99:13,885–13,896.

Brandon, M. T. 1996. Probability density plot for fission-track grain-age samples. Radiat. Meas. 26:663–676.

Brandon, M. T.; Roden-Tice, M. K.; and Garver, J. I. 1998. Late Cenozoic exhumation of the Cascadia accretionary wedge in the Olympic Mountains, northwest Washington state. Geol. Soc. Am. Bull. 110:985–1009.

Bullen, M. E.; Burbank, D. W.; Abdrakhmatov, K. Y.; and Garver, J. 2001. Late Cenozoic tectonic evolution of the northwestern Tien Shan: constraints from magnetostratigraphy, detrital fission track, and basin analysis. Geol. Soc. Am. Bull. 113:1544–1559.

Burbank, D. W.; McLean, J. K.; Bullen, M. E.; Abdrakhmatov, K. Y.; and Miller, M. G. 1999. Partitioning of intermontane basins by thrust-related folding, Tien Shan, Kyrgyzstan. Basin Res. 11:75–92.

Burtman, V. S. 1975. Structural geology of the Variscan Tien Shan. Am. J. Sci. 280:725–744.

———. 1980. Faults of middle Asia. Am. J. Sci. 275A: 157–186.

Burtman, V. S.; Skobelev, S. F.; and Molnar, P. 1996. Late Cenozoic slip on the Talas-Ferghana Fault, the Tien Shan, Central Asia. Geol. Soc. Am. Bull. 108: 1004–1021.

Carlson, W. D.; Donelick, R. A.; and Ketcham, R. A. 1999. Variability of apatite fission track annealing kinetics. I. Experimental results. Am. Mineral. 84:1213–1223.

Carroll, A. R.; Graham, S. A.; Hendrix, M. S.; Ying, D.; and Zhou, D. 1995. Late Paleozoic tectonic amalgamation of northwestern China: sedimentary record of the northern Tarim, northwestern Turpan, and southern Junggar basins. Geol. Soc. Am. Bull. 107: 571–594.

Chediya, O. K.; Abdrakhmatov, K. Y.; Lamzin, I. H.; Michel, G.; and Michailev, V. 1998. Seismotectonic characterization of the Issyk Ata fault. Bishkek, Institute Nauk Kyrgyzskoi, p. 58–69.

Chediya, O. K.; Yazovskii, V. M.; and Fortuna, A. B. 1973. O stratigraficheskom raschlenenii krasnotsvetnogo kompleksa v Chuyskoy vpadine I yeye gornom obramlenii (The stratigraphic subdivision of the Kyrgyz red-bed complex in the Chu basin and the surrounding mountains). *In* Zakonomernosti geologicheskogo razvitiya Tyan-Shanya v kaynozoye (Principles of the geologic development of the Tyan-Shan in the Cenozoi). Bishkek, Ilim, p. 26–52.

Cobbold, P. R.; Sadybaksov, E.; and Thomas, J. C. 1996. Cenozoic transpression and basin development. *In* Roure, F.; Ellouz, N.; Shein, V. S.; and Skvortsov, I. I., eds. Geodynamic evolution of sedimentary basins. Paris, Editions Technip, p. 181–202.

Crowley, K. D.; Cameron, M.; and McPherson, B. J. 1990. Annealing of etchable fission-track damage in F-, OH-, Cl-, and Sr-apatite. 1. Systematics and preliminary interpretation. Nucl. Tracks Radiat. Meas. 17: 409.

Farley, K. A. 2000. Helium diffusion from apatite: general behavior as illustrated by Durango fluorapatite. J. Geophys. Res. 105:2903–2914.

Farley, K. A.; Wolf, R. A.; and Silver, L. T. 1996. The

effects of long alpha-stopping distances on (U-Th)/He ages. Geochim. Cosmochim. Acta 60:4223–4229.

Fitzgerald, P. G.; Sorkhabi, R. B.; Redfield, T. F.; and Stump, E. 1995. Uplift and denudation of the central Alaska Range: a case study in the use of apatite fission track thermochronology to determine absolute uplift parameters. J. Geophys. Res. 100:20,175–20,191.

Galbraith, R. F., and Green, P. F. 1990. Estimating the component ages in a finite mixture. Nucl. Tracks Radiat. Meas. 17:197–206.

Garver, J. I.; Brandon, M. T.; Roden-Tice, M.; and Kamp, P. J. J. 1999. Erosional denudation determined by fission-track ages of detrital apatite and zircon. *In* Ring, U.; Brandon, M. T.; Willett, S.; and Lister, G., eds. Exhumation processes: normal faulting, ductile flow, and erosion. Geol. Soc. Lond. Spec. Publ. 154:283–304.

Ghose, S.; Mellors, R. J.; Korjenkov, A. M.; Hamburger, M. W.; Pavlis, T. L.; Pavlis, G. L.; Omuraliev, M.; et al. 1997. The Ms = 7.3 1992 Suusamyr, Kyrgyzstan, earthquake in the Tien Shan. 2. Aftershock focal mechanisms and surface deformation. Bull. Seismol. Soc. Am. 87:23–38.

Gleadow, A. J. W.; Duddy, I. R.; Green, P. F.; and Lovering, J. F. 1986. Confined fission track lengths in apatite: a diagnostic tool for thermal history analysis. Contrib. Mineral. Petrol. 94:405–415.

Green, P. F. 1981. A new look at statistics in fission-track dating. Nucl. Tracks Radiat. Meas. 5:77–86.

Green, P. F.; Duddy, I. R.; Laslett, G. M.; Hegarty, K. A.; Gleadow, A. J. W.; and Lovering, J. F. 1989. Thermal annealing of fission tracks in apatite. 4. Quantitative modelling techniques and extension to geological timescales. Chem. Geol. Isot. Geosci. Sect. 79: 155–182.

Green, P. F.; Duddy, I. R.; Laslett, G. M.; Hegarty, K. A.; Gleadow, A. J. W.; Tingate, P. R.; and Laslett, G. M. 1985. Fission track annealing in apatite: track length measurements and the form of the Arrhenius plot. Nucl. Tracks 10:233–253.

Hendrix, M. S.; Dumitru, T. A.; and Graham, S. A. 1994. Late Oligocene–Early Miocene unroofing in the Chinese Tian Shan: an early effect of the India-Asia collision. Geology 22:487–490.

Hendrix, M. S.; Graham, S. A.; Carroll, A. R.; Sobel, E. R.; McKnight, C. L.; Schulein, B. J.; and Wang, Z. 1992. Sedimentary record and climatic implications of recurrent deformation in the Tian Shan: evidence from Mesozoic strata of the north Tarim, south Junggar, and Turpan basins, northwest China. Geol. Soc. Am. Bull. 104:53–79.

Larson, K. M.; Bürgmann, R.; Bilham, R.; and Freymueller, J. T. 1999. Kinematics of the India-Eurasian collision zone from GPS measurements. J. Geophys. Res. 104:1077–1093.

Mancktelow, N. S., and Grasemann, B. 1997. Time-dependent effects of heat advection and topography on cooling histories during erosion. Tectonophysics 270:167–195.

Meigs, A. J. 1997. Sequential development of selected Pyrenean thrust faults. J. Struct. Geol. 19:481–502.

Mikolaichuk, A. B. 1999. Neotectonic faults of the Kyrghyz Range. J. Sci. New Tech. (in Russian) 2:42–47.

Molnar, P., and Deng, Q. D. 1984. Faulting associated with large earthquakes and the average rate of deformation in central and eastern Asia. J. Geophys. Res. 89:6203–6228.

Molnar, P., and England, P. 1990. Late Cenozoic uplift of mountain ranges and global climatic change: chicken or egg? Nature 346:29–34.

Molnar, P.; England, P.; and Martinod, J. 1993. Mantle dynamics, uplift of the Tibetan Plateau, and the Indian monsoon. Rev. Geophys. 31:357–396.

Molnar, P., and Tapponier, P. 1975. Cenozoic tectonics of Asia: effects of a continental collision. Science 189: 419–426.

Norin, E. 1941. Geologic reconaissances in the Chinese Tien Shan: reports from the scientific expedition to the northwest provinces of China under the leadership of Dr. Sven Hedin, (III), Geology 6. Stockholm, Aktiebolaget Thule, 229 p.

Patriat, P., and Achache, J. 1984. Indo-Asia collision chronology and its implications for crustal shortening and driving mechanisms of plates. Nature 311:615–621.

Reigber, C.; Michel, G. W.; Galas, R.; Angermann, D.; Klotz, J.; Chen, J. Y.; Papschev, A.; et al. 2001. New space geodetic constraints on the distribution of deformation in Central Asia. Earth Planet. Sci. Lett. 191: 157–165.

Roecker, S. W. 1999. New constraints on the crust and upper mantle of the Kyrgyz Tien Shan from analysis of GHENGIS broadband seismic data. EOS: Trans. Am. Geophys. Union 80:1017.

Roecker, S. W.; Sabitova, T. M.; Vinnik, L. P.; Burmakov, Y. A.; Golvano, M. I.; Mamatkanova, R.; and Munirova, L. 1993. Three-dimensional elastic wave velocity structure of the western and central Tian Shan. J. Geophys. Res. 98:15,779–15,795.

Shvartzman, Y. G. 1992. Thermal field, seismicity and geodynamics of the Tien Shan. Unpub. Ph.D. dissertation, University of Kyrgyzstan, Bishkek.

Small, E. E.; Anderson, R. S.; Hancock, G. S.; and Finkel, R. C. 1997. Estimates of regolith production from 10Be and 26Al: evidence for steady state alpine hillslopes. Geomorphology 27:131–150.

Sobel, E. R., and Dumitru, T. A. 1997. Thrusting and exhumation around the margins of the western Tarim basin during the Indian-Asia collision. J. Geophys. Res. 102:5043–5063.

Stock, J. D., and Montgomery, D. R. 1996. Estimating palaeorelief from detrital mineral age ranges. Basin Res. 8:317–328.

Stockli, D.; Farley, K. A.; and Dumitru, T. A. 2000. Calibration of the apatite (U-Th)/He thermochronometer on an exhumed fault block, White Mountains, California. Geology 28:983–986.

Stüwe, K.; White, L.; and Brown, R. 1994. The influence of eroding topography on steady-state isotherms: application to fission track analysis. Earth Planet. Sci. Lett. 124:63–74.

Thompson, S. C.; Weldon, R., III; Rubin, C. M.; Abdrakh-

matov, K.; Molnar, P.; and Berger, G. W. 2002. Late Quaternary slip rates across the central Tien Shan, Kyrgyzstan, Central Asia. J. Geophys. Res. 107(B9), doi:10.1029/2001JB000596, 2002.

Trofimov, A. K.; Udalov, H. P.; Utkena, H. G.; Fortuna, A. B; Chediya, O. K.; and Yazovski, B. M. 1976. Geologiya kaynozoya Chuyskoy vpadini i eyo gornogo obramleniya (Cenozoic geology of the Chuysk basin and surrounding mountains). Leningrad, Academia Nauk CCP, 128 p.

Wang, Q.; Guoyu, D.; Xuejun, Q.; Xiaoqiang, W.; and Xinzhao, Y. 2000. Recent rapid shortening of crust across the Tianshan Mts. and relative motion of tectonic blocks in the north and south. Chin. Sci. Bull. 45:1995–1999.

Whipple, K. E.; Kirby, E.; and Brocklehurst, S. H. 1999. Geomorphic limits to climate-induced increases in topographic relief. Nature 401:39–43.

Windley, B. F.; Allen, M. B.; Zhang, C.; Zhao, Z.-Y.; and Wang, G.-R. 1990. Paleozoic accretion and Cenozoic redeformation of the Chinese Tien Shan Range, Central Asia. Geology 18:128–131.

Wolf, R. A.; Farley, K. A.; and Kass, D. M. 1998. Modeling of the temperature sensitivity of the apatite (U Th)/He thermochronometer. Chem. Geol. 148:105–114.

Yin, A.; Nie, S.; Craig, P.; Harrison, T. M.; Ryerson, F. J.; Xianglin, Q.; and Geng, Y. 1998. Late Cenozoic tectonic evolution of the southern Chinese Tien Shan. Tectonics 17:1–27.

Zhang, P.; Molnar, P.; and Downs, W. R. 2001. Increased sedimentation rates and grain sizes 2–4 Myr ago due to the influence of climate change on erosion rates. Nature 410:891–897.

Zheng, H.; Powell, C. M.; An, Z.; Zhou, J.; and Dong, G. 2000. Pliocene uplift of the northern Tibetan Plateau. Geology 28:715–718.